Electronic Supplementary Material (ESI) for ChemComm.

Supplementary Information

Defective ATP breakdown activity related to an ENTPD1 gene mutation demonstrated using ^{31}P NMR

Atara Nardi-Schreiber[1], Gal Sapir[1], Ayelet Gamliel[1], Or Kakhlon[2], Jacob Sosna[1], J. Moshe Gomori[1], Vardiella Meiner[3], Alexander Lossos[#2], and Rachel Katz-Brull[#1]

Departments of Radiology[1], Neurology[2], and Genetics[3]

Hadassah-Hebrew University Medical Center

[#] Equal contribution

Materials, methods, results, and discussion not included in the main text

Table of Contents

Chemicals

ATP as adenosine 5'-triphosphate disodium salt was obtained from Sigma-Aldrich (Rehovot, Israel). All other chemicals used were of analytical grade and of the highest purity. Ficoll was obtained from GE healthcare (Ficoll-Paque Plus, Uppsala, Sweden). Tris-HCl buffer was prepared by titrating 50 mM Tris solution with HCl to a pH of 8.

^{1}H NMR spectroscopy in body fluids – methods and results

Urine and plasma samples were scanned by ^{1}H-NMR at 11.8 T (Varian, Agilent, The Netherlands). The samples were first scanned at pH 2.5 in order to confirm assignments with the standards of the Radboud laboratory [1] and enable comparison to other previously reported metabolic disorders [1, 2]. These spectra did not show evidence of ATP, ADP, or thymidine triphosphate. Then the samples were spiked with these compounds, confirming the ability to visualize these metabolites in the sample and confirming the lack of accumulation of these compounds in the plasma and urine of the family members.

Then the samples were scanned again at pH 7 to look for similarities of unidentified signals in our samples to ^{1}H spectra of other relevant compounds on the Human Metabolome Data Base (HMDB) [3] (searchable by ^{1}H chemical shift, whereas ^{1}H spectra of water soluble compounds appear at pH 7). In this way we searched for evidence of the following specific compounds in the samples: AMP, guanosine triphosphate, and citidine triphosphate. We did not detect signals at chemical shifts that would indicate the existence of these compounds in the samples.

Other purine/pyrimidine signals that could indicate a purine/pyrimidine metabolic disorder were also searched for. A standard human urine sample spiked with purine/pyrimidine metabolites and intermediates was purchased from MCA laboratory (SKML, Control Purines&Pyrimidines, Winterswijk, The Netherlands) and scanned at the same conditions. This sample served as a standard for the chemical shifts and detection limits of these spiked metabolites and intermediates. Using this reference urine sample containing purines and pyrimidines standards, the following compounds were specifically searched for but were not detected in the family urine or plasma: hypoxantine, adenosine, deoxyadenosine, uracil, thymidine, uridine, xantine, thymine, orotic acid, deoxyguanosine, deoxyinosine, inosine, guanosine, orotidine, 5-OH methyluracil, dihydro-uracil. In summary, we could not detect any evidence to purine/pyrimidine aberrant metabolism in the urine or the plasma samples of the family members.

Isolation of mononuclear cells from human blood

From each subject, about 20 ml of blood were collected in 6 standard heparinized vacutainers. Mononuclear cells were separated on Ficoll density gradients as described by Böyum [4] and by the manufacturer [5]. The blood in the heparinized tubes was combined to 10 ml batches which were processed in the following way: 10 ml of whole blood was mixed with 10 ml of medical grade saline (0.9% v/v sodium chloride) and the mixture was then gently placed above 20 ml of Ficoll in a 50 ml tube. After centrifugation (20 min at 800 x g), the middle whitish layer was collected and combined to one sample per subject. The cells were then washed twice with saline at room temperature with the same centrifugation duration at 400 x g.

Complete blood count determination

A complete blood count was performed in the central laboratory of Hadassah-Hebrew University Medical Center (COULTER LH-750 Hematology Analyzer) using standard protocols. The mononuclear cell count in the samples ranged between 31-59 million cells per sample.

E-NTPDase enzyme activity

Activity assay

The E-NTPDase activity of the subjects' mononuclear cells phase was investigated using reaction conditions that were previously described by Leal *et al.* [6] and Souza *et al.* [7] and were adjusted here for the sensitivity requirements of ^{31}P-NMR detection on our NMR system. The reaction medium contained 0.5 mM $CaCl_2$, 120 mM NaCl, 5 mM KCl, 60 mM glucose, and 50 mM Tris–HCl buffer. First, the mononuclear cells were suspended and pre-incubated in this reaction medium (final volume of 1,250 µl) for 10 min at 37 °C. Then, 2.45 or 8 µmol of ATP (resulting in a final concentration of 2.0 or 6.4 mM) was added to the incubation medium (which contained the cells) and incubation continued at shift rotation for 60 minutes at 37 °C. The reaction was halted by placing the sample in an ice-water bath. This was followed by quick heating of the entire sample for 10 min in an 80 °C water bath. The last step was performed in order to denature all proteins and irreversibly stop the reaction without degrading the high-energy tri- and di-phosphate compounds.

Sample preparation for NMR analysis

The heated samples were allowed to cool and then centrifuged at 2,700 x g for 5 min. The supernatant was aspirated and the cellular debris residue was kept for protein content determination. Phenylphosphonic acid (PPA, 80 µl of 100 mM solution), D_2O (300 µl), and purified water were added to the supernatant to a total volume of 3 ml with 2.7 mM PPA and 10 % D_2O. PPA served as an internal concentration reference and D_2O was added to enable locking of the magnetic field in the NMR spectrometer. The resulting solution was titrated to a pH of 7 using NaOH and transferred to a 10 mm NMR tube.

Protein content determination

The amount of protein in each sample was determined using the Bradford assay [8]. The assay utilizes an acidic solution of Coomassie Brilliant Blue G-250 (Bio-Rad, Israel) dye which binds to protein amino acid residues. The cellular debris residue which was left from the reaction step was combined with a lysis solution (Reporter lysis buffer, Promega, Israel) to a total volume of 1.5 ml. SDS 1% (150 µl) was added for a 15 min incubation. Then, 20 µl of this mixture was reacted with 1 ml of the Bradford reagent. After 30 minutes, the absorbance was read at 595 nm. The amount of protein was determined using a calibration curve (0-1.4 mg/ml) obtained using bovine serum albumin at known concentrations. The range of protein content in the samples investigated here was 0.24 to 0.46 mg per subject.

^{31}P-NMR spectroscopy

^{31}P-NMR recordings were carried out on a 5.8 Tesla high-resolution NMR spectrometer (RS^{2}D, Mundolsheim, France) with a 10 mm direct multinuclei probe at 22 °C. The reactions data were recorded in a steady state of magnetization using a repetition time of 2 s, nutation angle of 45 °, bandwidth of 10 kHz, and 8,912 points. The total number of excitations ranged between 20,000 and 32,768 resulting in a total scan time of about 8 to 18 h. To correct for relaxation effects, a sample of one of the healthy volunteers was recorded under fully relaxed conditions using a repetition time of 91 s and a nutation angle of 90 °. The total number of excitations was 2,080 resulting in a total scan time of *ca.* 52.5 h. The relative intensity ratios in the steady-state and fully relaxed spectra of that volunteer served to correct for relaxation effects in the quantification of ATP, ADP, AMP, and Pi *vs.* the PPA concentration standard in the complete data set.

The percent error of each compound was based on its signal to noise ratio in the fully relaxed spectrum (which showed the lowest SNR of all the acquisitions described herein).

^{31}P NMR spectra of standard solutions for signal assignments were acquired in a steady state of magnetization using a repetition time of 10 s, nutation angle of 90 °, bandwidth of 8 kHz, and 8,912 points. The total number of excitations was 640 resulting in a total scan time of about 1.8 h.

To determine the potential effect of a higher magnetic field on the spectral resolution and the scan time, two samples were scanned in an 11.8 T spectrometer equipped with a 5 mm PABBO probe (Bruker, Billerica, MA, USA). The same acquisition conditions were used expect for the number of excitations. The number of excitations used for the volunteer sample was 2048 (total scan time of 68 min), and the standard solution was acquired with 160 excitations (total scan time of 26 min).

Spectral post-processing and analysis were carried out using MNova (Mestrelab Research, Santiago de Compostela, Spain). The spectra were processed by applying an exponential function with a line-broadening factor of 7 Hz and zero filling to 32,768 points prior to Fourier transformation, followed by manual phasing, baseline correction, and integration. The α-ATP signal at δ=-10.03 ppm was used as chemical shift reference.

Assignment of phosphates signals on ^{31}P NMR spectra – standard samples

Figure 1 demonstrates ^{31}P spectra acquired from standard phosphate samples. The resolution of the signals attributed to ATP, ADP, AMP, and Pi on such spectra is clearly visible.

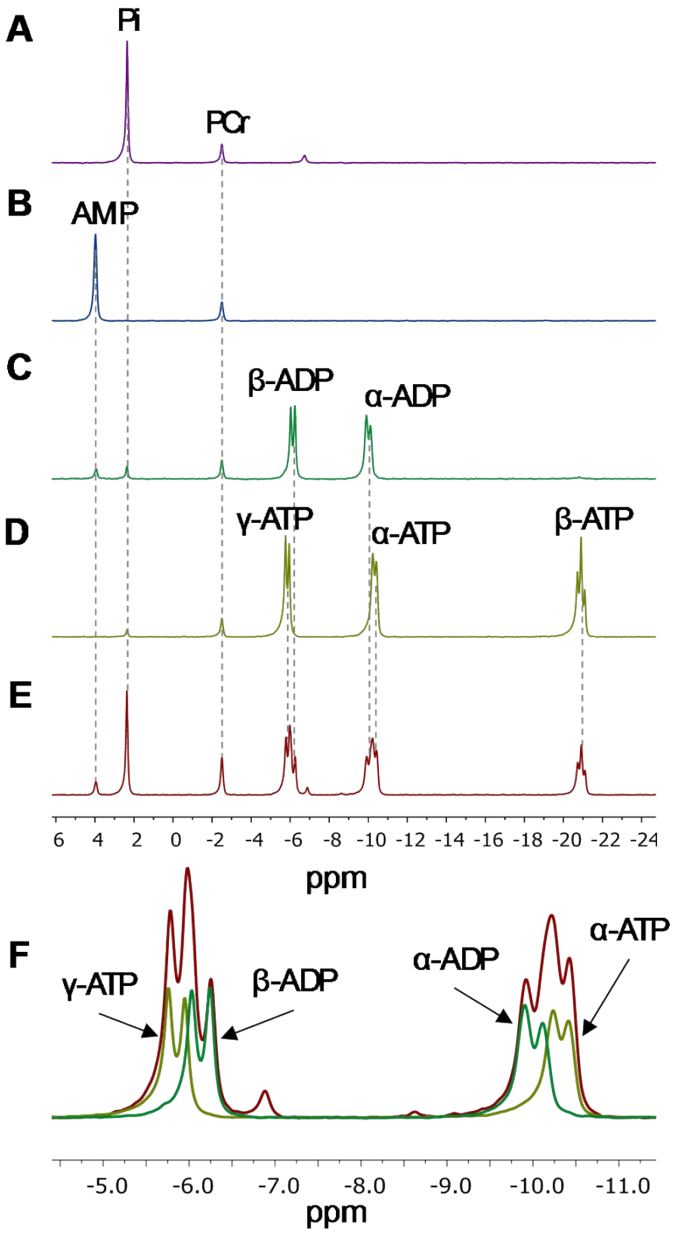

Figure 1. ^{31}P NMR spectra of phosphate standard samples.
A) 40 mM Pi and 10 mM PCr.
B) 40 mM AMP and 10 mM PCr.
C) 40 mM ADP and 10 mM PCr (contaminations of AMP and Pi are observed at the relevant chemical shifts shown in A and B). The line-width at half height of the β-ADP signals was 3.75 ± 0.25 Hz.
D) 40 mM ATP and 10 mM PCr (a contamination of Pi is observed at the chemical shift shown in A). The line-width at half height of the γ-ATP signals was 3.8 ± 0.2 Hz.
E) 10 mM of Pi, AMP, ADP, ATP, and PCr.
F) An expanded ^{31}P spectrum shows the region of the γ-ATP ,β-ADP, α-ATP and α-ADP signals. The red line shows the mixed sample (E); The light green line shows the ATP sample (D); and the dark green line shows the ADP sample (C).
PCr, phosphocreatine; AMP, adenosine monophosphate; Pi, inorganic phosphate; ATP, adenosine triphosphate; ADP, adenosine diphosphate. The chemical shift was

calibrated using PCr at -2.5 ppm [9]. Spectra A-F were processed with an exponential multiplication (line-broadening) of 7 Hz.

Calibration graph for ATP determination using ^{31}P NMR spectroscopy

Sample preparation: A sample of 11.5 mM ATP and 1.35 mM PCr in medical grade saline solution (0.9% v/v NaCl) was prepared with 20 mM of phenylphosphonic acid (PPA). The pH was adjusted to 7 and D_2O was added (to 10 %). This sample was then diluted using a mixture of 90 % medical grade saline and 10 % D2O titrated to pH 7 prior to dilution. Four repeated dilutions of 2, 2.5, 2, and 2 fold resulted in ATP sample concentrations of 11.5, 5.75, 2.3, 1.15, 0.575 mM, and PCr sample concentrations of 1.35, 0.675, 0.27, 0.135, 0.0675 mM, respectively.

NMR data acquisition: The data for the calibration graph were recorded under steady-state conditions using a repetition time of 2 s, nutation angle of 45 °, bandwidth of 8 kHz, and 8,912 points. These are the same acquisition conditions used for acquiring the experimental data in the text (described above). The number of excitations ranged between 1,200 and 28,800 resulting in a total scan time of *ca.* 0.33 to 16 h, where more excitations were required to achieve good SNR at the lower concentrations (of equivalent concentration to the experimental data).

Relaxation effects were corrected using a fully relaxed spectrum of the sample with the highest concentration of ATP (11.5 mM). The acquisition conditions for this fully relaxed spectrum were: repetition time of 90 s, nutation angle of 90 °, and 600 excitations (scan time *ca.* 15 h).

The concentration of ATP and PCr as determined by ^{31}P spectroscopy of the samples, is presented in Figure 2. The values for ATP reflect an averaged value determined from the three signals of α-ATP, β-ATP, and γ-ATP. The individual quantification per each of these signals is shown in Table 1. The slope of the linear fit of the data (Figure 2) was 0.99 and 1.04 for ATP and PCr, respectively, suggesting that the ^{31}P NMR spectroscopy approach described herein is useful and appropriate for the quantification of phosphate containing compounds at the concentration range present in the reaction samples.

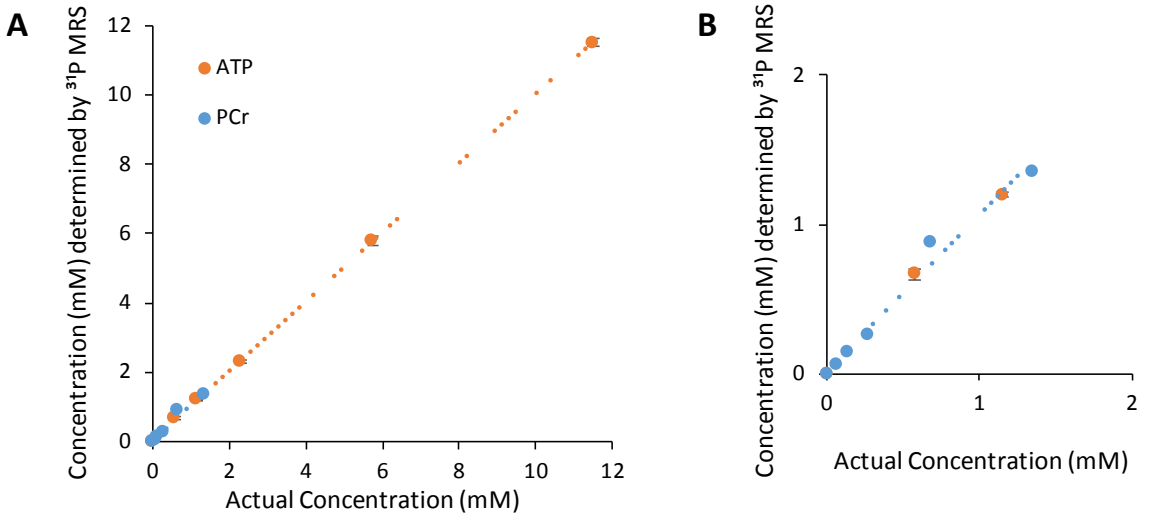

Figure 2. Concentration determination of phosphate containing compounds (ATP and PCr) using ^{31}P NMR.

A) the full range of concentrations investigated here. B) expansion of the 0 - 2 mM range. Sample preparation, NMR acquisition, and the quantification procedures are described above. The linear fit for the ATP data was $y = 0.9977x + 0.043$, $R^2 = 0.9999$. The linear fit for the PCr data $y = 1.0416x + 0.0155$, $R^2 = 0.9763$.

Error bars for ATP quantification were calculated using standard deviation of the results shown in Table 1. *i.e.* the quantification of ATP *via* its three signals. The error values were less than 2.1 % of the main value and are therefore not visible on the graph.

Table 1. Quantification of ATP based on each of the 3 phosphate signals.

	Sample 1	Sample 2	Sample 3	Sample 4	Sample 5
Actual ATP concertation in the sample (mM)	11.50	5.75	2.30	1.15	0.575
Quantification based on the α-ATP signal (mM)	11.65	5.93	2.37	1.20	0.71
Quantification based on the β-ATP signal (mM)	11.43	5.63	2.27	1.18	0.63
Quantification based on the γ-ATP signal (mM)	11.46	5.81	2.31	1.22	0.66
Quantification based on the 3 ATP signals (average ± standard deviation, mM)	11.51 ± 0.10	5.79 ± 0.12	2.32 ± 0.04	1.20 ± 0.02	0.67 ± 0.03

^{31}P NMR quantification of ADP and ATP in the human mononuclear cell reaction samples

The β-ATP signal was fully resolved at ~ -20 ppm. However, the signals of ADP (α and β) appear at a chemical shift which is very close to the signals of ATP (α and γ), at ~ -10 and ~-5 ppm, respectively. In the spectra processed as above these signals slightly overlap (Figure 3B), prohibiting accurate quantification of ADP. In principle, the ADP content may be obtained by subtraction of the β-ATP signal integrated intensity from that of either the signal at -5 or -10 ppm. However, due to the noise in these measurements, such an approach led to inconsistent results. Therefore, to resolve and quantify ADP, the spectra were also processed in two additional ways:

1) The spectra were processed with a line-broadening of 0.5 Hz. In this way, the γ-ATP and β-ADP peaks were resolved (Figure 3A) albeit with a lower signal-to-noise ratio. The relative integrated intensities of γ-ATP and β-ADP were determined. Then, this ratio was used for ADP quantification in the spectra processed with a 7 Hz line-broadening factor.

2) The γ-ATP and β-ADP signals were simulated with a line-broadening of 7 Hz (Figure 3B). A fit of this simulation to the individual spectra provided the ratio between γ-ATP and β-ADP. Then, this ratio was used for ADP quantification. The results obtained by either approach were similar with a correlation factor of 0.99. The results of the first approach, *i.e.* the relative integrals of the γ-ATP and β-ADP for each subject, in spectra processed with a low line-broadening factor, were used in the final analysis.

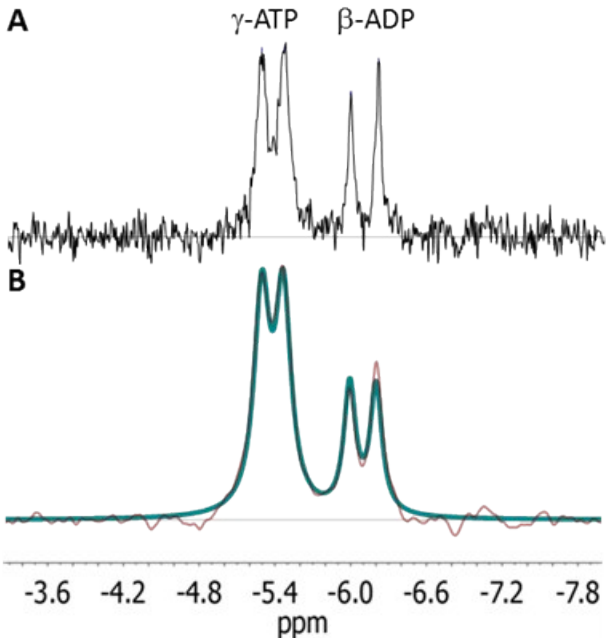

Figure 3. Quantitative determination of γ-ATP to β-ADP ratio by ^{31}P NMR.
A) Determination by high resolution processing and integration: An expanded ^{31}P spectrum shows the region of the γ-ATP and the β-ADP signals. This spectrum was processed with an exponential multiplication (line-broadening) of 0.5 Hz. Because the signals are well resolved, integration could be applied for quantification, resulting in a 1:0.47 ratio, respectively. The line-width at half height of the γ-ATP signals was 10.5 ± 0.3 Hz. The line-width of the β-ADP signals was 3.55 ± 0.45 Hz. B) Determination of the γ-ATP to β-ADP ratio by simulation. The red line shows the actual spectrum processed with a line-broadening of 7 Hz. The green line depicts a simulation of these signals, which resulted in a ratio of 1:0.45, respectively.

Further quantification of ATP, ADP, AMP and Pi in the reaction with human mononuclear cells

ATP, ADP, AMP, and Pi concentrations degraded/produced in the reaction of human mononuclear cells with ATP were determined in the sample tube as described above. Further quantification of these metabolites was performed in two ways: 1) The concentrations were normalized per mg protein achieved from the protein content determination for each subject; and 2) The concentrations were normalized per mononuclear cell count achieved from the complete blood count determine for each subject. The results are presented in the main text.

Statistical analysis

^{31}P-NMR data are expressed as mean ± 20 % in agreement with the signal-to-noise of the measurements (upper error limit). Correlation was analyzed with the corresponding function in Excel (Microsoft Office 2013).

Comparison of the spectral resolution and the acquisition times in a higher magnetic field (11.8 T)

Figure 4 demonstrates the differences in spectral resolution and scanning times obtained in a higher magnetic field of 11.8 T (all of the other data presented herein and in the text were obtained at 5.8 T). At 11.8 T, the available ^{31}P probe was of 5 mm, as opposed to the 5.8 T spectrometer which was equipped with a 10 mm probe. This leads to much improved sensitivity of the 11.8 T spectrometer set-up (which is a widely available set-up in many institutions). Figure 4A and 4B demonstrate the ^{31}P spectra of one of the standard samples (also shown in Figure 1E), recorded in the two set-ups. The standard solution measurements were recorded with the same acquisition parameters (described above under ^{31}P-NMR spectroscopy) except for the number of excitations (640 and 160 at 5.8 T and 11.8 T, respectively). The resulting SNR was 5 times greater at 11.8 T, despite the four-fold decrease in scan time and despite the fact that the actual amount of ^{31}P nuclei was reduced about 6 fold due to the use of 5 mm instead of 10 mm NMR tubes.

The same effects can be appreciated in the recordings of one of the reaction samples from one of the volunteers shown in Figure 4C and 4D, recorded at 5.8T and 11.8 T, using 8192 and 2048 excitations, respectively. Other acquisition parameters are described above (under ^{31}P-NMR spectroscopy). The SNR was two-folds greater at 11.8 T despite the four-fold decrease in scan time and despite the approximate 6-fold decrease in content due to the use of 5 mm tubes as described above.

In principle, the reaction described herein could have been performed in smaller reaction volumes. Considering such a reduction of sample in volume (and thus an increase of about 6 fold in phosphates concentration), the scanning time could have been shortened 36 fold. Hence, the scanning time of about 8 h for the samples described herein could have been shortened to about 13 min. Considering also that the SNR at 11.8 T was 5 fold higher, settling for the SNR presented at 5.8 T, the scan time could have been further shortened by at least another order of magnitude. This brings the potential scan time of typical samples of ENTPDase activity of human mononuclear cells to the order of single minutes, in a high magnetic field spectrometer equipped with a high sensitivity probe. In this way, the work

presented here sets a baseline for an efficient approach to phosphate metabolomics research, and presents the limits of detection set by instrumental parameters.

We note that the greater signal intensity ratio of AMP-to-ADP and AMP-to-ATP observed at 11.8 T (Figure 4B compared to 4A and 4D compared to 4C) likely reflects a shorter T_1 of AMP compared to ADP or ATP at the higher magnetic field. T_1 relaxation properties were not determined in the current study and likely depend on the particular magnetic field used and the specific sample composition and concentrations.

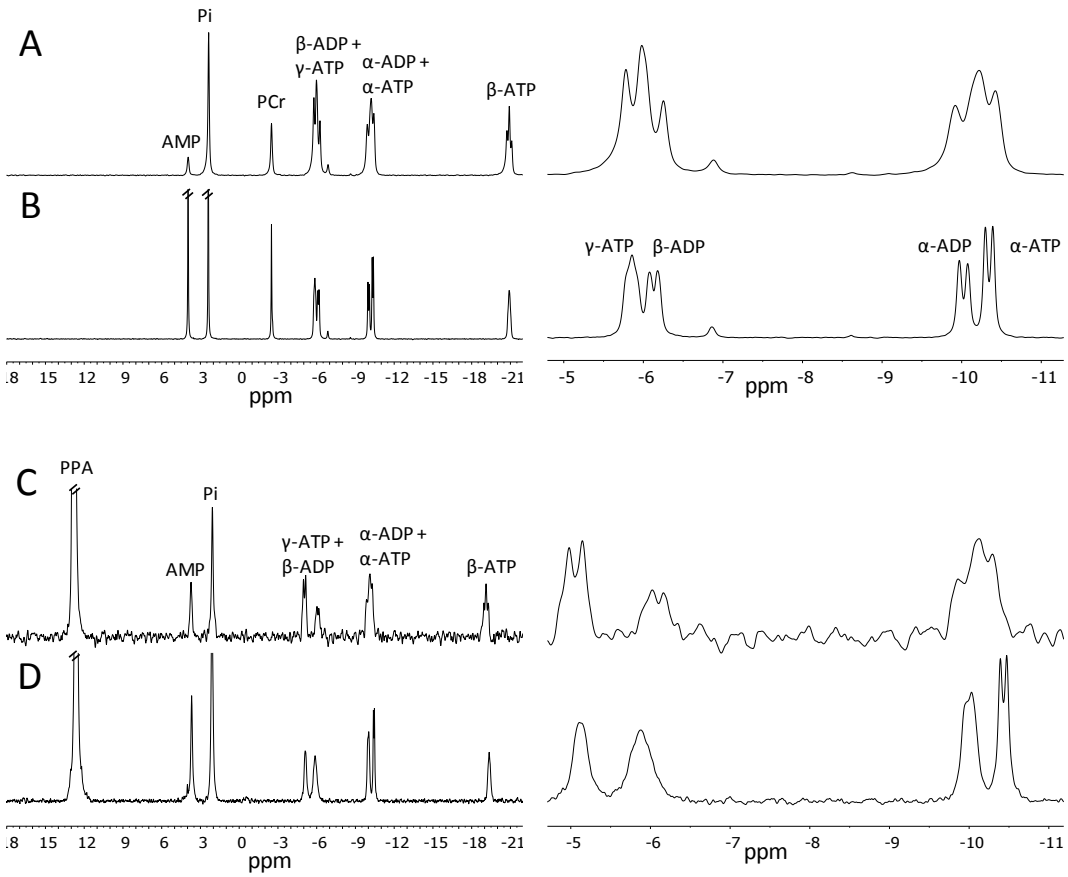

Figure 4. The effect of a higher magnetic field on the spectral resolution and the scanning time of ^{31}P NMR spectra of samples from the current study.

The right hand side shows an expansion of the chemical shift range of -5 to -11 ppm.

A) A standard solution of 10 mM of Pi, AMP, ADP, ATP, and PCr recorded at 5.8 T, 64 min acquisition time.

B) The same standard solution as in A, recorded at 11.8 T, 16 min acquisition time.

C) A reaction sample of one of the volunteers' mononuclear cells recorded at 5.8 T, 4.55 h acquisition time.

D) The same sample as in C, recorded at 11.8 T, about 1.14 h acquisition time.

All of the spectra were processed with a line-broadening of 7 Hz.

The increase in spectral resolution is evident in spectra B and D, which demonstrate a clear separation between the signals of ATP and ADP. This is due to the fact the J-coupling constants (constant in Hz) span a smaller range in the chemical shift (ppm) scale at the higher filed. This leads to less of an overlap between the corresponding doublet signals.

^{1}H-NMR spectroscopy of standard samples and reaction samples- for the reaction of ATP with human mononuclear cells

^{1}H-NMR recordings were carried out on a 5.8 Tesla high-resolution NMR spectrometer (RS^{2}D, Mundolsheim, France) with a 5 mm ^{1}H/^{13}C double tuned probe at room temperature. Two samples were investigated: a standard sample and a sample of ATP breakdown reaction by mononuclear cells from one of the healthy volunteers.

The standard sample contained ATP, ADP, AMP, PI, and PCr, all at a concentration of 10 mM in 90:10 H_2O:D_2O. The sample from the healthy volunteer was originally scanned for ^{31}P NMR spectroscopy in a total volume of 3 ml and an upper limit for the ATP concertation of 0.83 mM (2 mM added the reaction volume of 1,250 μl diluted to 3 ml for ^{31}P-NMR). For ^{1}H-NMR spectroscopy, the sample was then lyophilized to dryness and then dissolved in 0.5 ml D_2O. Thus, the upper limit for ATP in the resulting sample was 5 mM. According to the ^{31}P NMR spectroscopy result, the breakdown process led to about 21:16:28 ATP:ADP:AMP in this sample.

Figure 4 demonstrates the relevant spectral regions for the identification and quantification of ATP, ADP and AMP on a ^{1}H-NMR spectrum.

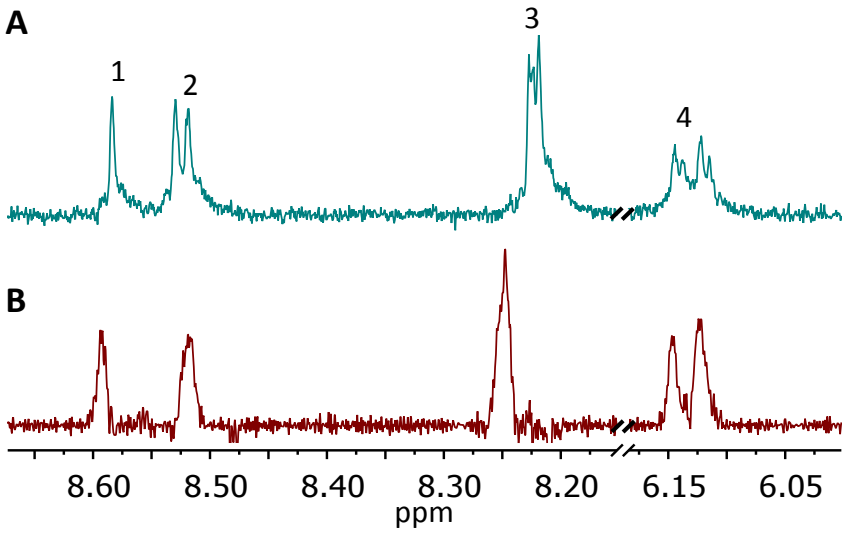

Figure 4. ^{1}H-NMR characteristic of ATP, ADP, and AMP.
An expanded ^{1}H spectrum shows the region of the adenine ring proton signals: 1, AMP; 2 ATP and ADP; 3, ATP, ADP, and AMP, and the region of the ribose proton signals (on the glycosidic bond) 4, ATP, ADP, and AMP.
A) A standard sample containing ATP, ADP, AMP, PI, and PCr, all at a concentration of 10 mM in 90:10 H_2O:D_2O, pH 7.
B) A sample obtained from the reaction of ATP and mononuclear cells of a healthy volunteer (lyophilized and re-dissolved in D_2O), pH 7. The composition of ATP, ADP, and AMP in this sample was determined by ^{31}P NMR and is described above.
Both spectra were acquired with 256 excitations, 45 ° nutation angle, repetition time of 7 s (scan time *ca.* 30 min), bandwidth of 6 kHz, and a presatNOE pulse sequence. Both spectra were processed with a line-broadening of 0.1 Hz and referenced to the ribose proton (on the glycosidic bond, signal 4) of ATP, ADP, and AMP at 6.125 ppm. This assignment is based on the assignment of this signal in HMDB for ATP and AMP in D_2O at pH 7 [10, 11]. The line-width at half-height of signal 1 of AMP was 1.01 Hz in spectrum A and 1.99 Hz in B.

The chemical shift difference observed here in the standard sample between the proton marked 2 (Figure 4) of ADP and ATP was 0.011 ppm (2.94 Hz). This difference is in agreement with a previous study which found this difference to be 0.01 ppm [12].
However, it is clear that the chemical shifts of signals 1, 2, and 3 changes slightly in the sample obtained from the reaction of mononuclear cells (Figure 4B). This slight change, possibly combined with a small increase in line widths, led to an inability to differentiate ADP and ATP based on signal 2 in mononuclear cells sample.

Other methods in use for determinations of ATP, ADP, AMP, and Pi which can be used to determine ENTPDase activity

There are several methods which have been used or can be used to detect E-NTPDase activity or NTP/NDP breakdown: 1) determination of NDP or NMP formation; 2) determination of NTP or NDP consumption; and 3) determination of Pi production. These determinations involve assays that are based on luminescence [13, 14], colorimetry [15-19], radioactivity [20, 21], high-performance liquid chromatography (HPLC) [22], ion chromatography [23], and negative ion electrospray tandem mass spectrometry (ESI-MS/MS) [24]. Of specific note are the HPLC based methods which consist of reverse-phase columns with basic ion-pairing groups which are able to separate adenosine nuclotides. Provided these columns, HPLC can provide fast and accurate information on small amounts of ATP, ADP, AMP, and other nucleotides [25]. For example: Moritz *et al.* [22] have shown the quantification of ATP, ADP, and AMP in blood serum using HPLC. However, to quantify Pi, the authors [22] have used the malachite green colorimetric assay [18]. Ozkok [26] *et al.* have shown the quantification of ATP, ADP, and AMP in muscle tissue using HPLC as well. Hill *et al.* [27] performed Pi quantification using an HPLC system. However, the Pi was not determined directly, rather, it was detected *via* its enzymatic phosphorylation reaction with thymidine to from 2-deoxyribose 1-phosphate. On the other hand, Gao *et al.* [23] have used ion chromatography to determine in one sample ATP, ADP, and Pi. Another way to microquantification of Pi was described by Safian *et al.* [24]. Their approach was based on negative ion electrospray tandem mass spectrometry and stable isotope dilution by $^{18}O_4$-labeled phosphate. Katz *et al.* [19] have shown the way to improve the colorimetric assay for determination of Pi by separating the Pi from other organic phosphate compounds prior to reaction with the molybdic acid. To the best of our knowledge, all four metabolites- ATP, ADP, AMP, and Pi cannot be determined in the same sample, with the same assay (or with the same column). Nevertheless, in principle, the use of multiple columns, assays, or appropriate controls could enable the determination of all three relevant process of the breakdown of ATP with human mononuclear cells.

References

1. U. F. H. Engelke, L. A. J. Kluijtmans, M. Huigen, A. Goudswaard, M. van der Graaf, A. Heerschap, E. Morava-Kozicz, S. Wortmann-Hagemann and R. A. Wavers, *Third Ed: Radboud University Medical Center*, 2014.
2. R. A. Wevers, U. F. Engelke, S. H. Moolenaar, C. Brautigam, J. G. de Jong, R. Duran, R. A. de Abreu and A. H. van Gennip, *Clin Chem*, 1999, **45**, 539-548.
3. Human Metabolome Data Base. http://www.hmdb.ca/metabolites (Accessed December 2016)).
4. A. Boyum, *Scand J Clin Lab Invest Suppl*, 1968, **97**, 77-89.
5. General Electric Healthcare. Ficoll-paque plus. https://www.gelifesciences.com/gehcls_images/GELS/Related%20Content/Files/1353593752833/litdoc18115269_20161015161132.pdf (Accessed December 2016), (accessed December 2016).
6. D. B. Leal, C. A. Streher, T. N. Neu, F. P. Bittencourt, C. A. Leal, J. E. da Silva, V. M. Morsch and M. R. Schetinger, *Biochim Biophys Acta*, 2005, **1721**, 9-15.
7. C. Souza Vdo, K. B. Schlemmer, C. B. Noal, J. A. Jaques, C. E. Zimmermann, C. A. Leal, J. Fleck, E. A. Casali, V. M. Morsch, M. R. Schetinger and D. B. Leal, *Parasitol Int*, 2012, **61**, 690-696.
8. M. M. Bradford, *Anal Biochem*, 1976, **72**, 248-254.
9. W. Voelter, K. Zech, P. Arnold and G. Ludwig, *J Chromatography*, 1980, **199**, 345-354.
10. HMDB, 1H NMR Spectrum of ATP, http://www.hmdb.ca/spectra/nmr_one_d/1411, (accessed 6/8, 2017).
11. HMDB, 1H NMR Spectrum of AMP, http://www.hmdb.ca/spectra/nmr_one_d/1051, (accessed 6/8, 2017).
12. B. Guo, P. S. Gurel, R. Shu, H. N. Higgs, M. Pellegrini and D. F. Mierke, *Chem Commun*, 2014, **50**, 12037-12039.
13. G. A. Kimmich, J. Randles and J. S. Brand, *Anal Biochem*, 1975, **69**, 187-206.
14. M. Brune, J. L. Hunter, J. E. Corrie and M. R. Webb, *Biochemistry*, 1994, **33**, 8262-8271.
15. Z. L. Wu, *PLoS One*, 2011, **6**, e23172.
16. J. Feng, Y. Chen, J. Pu, X. Yang, C. Zhang, S. Zhu, Y. Zhao, Y. Yuan, H. Yuan and F. Liao, *Anal Biochem*, 2011, **409**, 144-149.
17. K. Itaya and M. Ui, *Clin Chim Acta*, 1966, **14**, 361-366.
18. K. M. Chan, D. Delfert and K. D. Junger, *Anal Biochem*, 1986, **157**, 375-380.
19. F. E. Katz, X. Shi, C. P. Owens, S. Joseph and F. A. Tezcan, *Anal Biochem*, 2017, **520**, 62-67.
20. D. M. Berman, T. M. Wilkie and A. G. Gilman, *Cell*, 1996, **86**, 445-452.
21. S. Mukhopadhyay and E. M. Ross, *Proc Natl Acad Sci U S A*, 1999, **96**, 9539-9544.
22. C. E. J. Moritz, B. C. Teixeira, L. Rockenbach, A. Reischak-Oliveira, E. A. Casali and A. M. O. Battastini, *Mol Cell Biochem*, 2017, **426**, 55-63.
23. R. C. Gao, C. H. Xue, L. Yuan, Z. J. Li, Y. Xue, F. Cui and Y. Sun, *J Chromatogr A*, 2006, **1118**, 278-280.
24. M. F. Safian and W. D. Lehmann, *Anal Bioanal Chem*, 2015, **407**, 2933-2937.
25. S. Zur Nedden, R. Eason, A. S. Doney and B. G. Frenguelli, *Anal Biochem*, 2009, **388**, 108-114.
26. E. Ozkok, H. Yorulmaz, G. Ates, A. Aksu, N. Balkis, O. Sahin and S. Tamer, *Physiol Res*, 2016, **65**, 833-842.
27. Y. Yang and X. Geng, *J Chromatogr A*, 2011, **1218**, 8813-8825.